Development of an Implantable Light Emitting Diode Device for the Photoconversion and Photoactivation of KikGR33 and Ai32 Mouse Models

[a] Hanna Rainiero*, [a] Jacky Tian*, [a] Ruochen Wang* , [a] Lisa Xiong*

[a] Department of Biomedical Engineering, University of Wisconsin-Madison, Engineering Centers Building, 1550 Engineering Drive, Madison, WI 53706

* *Denotes co-first author*

Corresponding Author
Lisa Xiong
Biomedical Engineering
Department of Biomedical Engineering, University of Wisconsin-Madison, Engineering Centers Building, 1550 Engineering Drive, Madison, WI 53706
pxiong55@wisc.edu

Abstract

Background

Tuberculosis (TB) is a serious infectious disease with an increasing presence of antibiotic resistance further threatening populations. There are increased research efforts to understand how the immune system responds to TB. Two mouse models, KiGR33 and Ai32, are used to investigate immune cell trafficking as an alternative therapeutic target using photoconversion and optogenetic activation of immune cells utilizing photoactivation. KikGR mouse cells can be photoconverted from green to red when exposed to a 405 nm wavelength light and Ai32 mouse cells can be photoactivated when exposed to a 450-490 nm wavelength range. The current method for photoconversion/photoactivation involves a fiber optic cable with a needle attachment which lacks surface area exposure necessary for efficient photoconversion or photoactivation.

New Method

Light emitting diodes (LEDs) will be used to photoconvert and photoactivate the mouse model cells. A printed circuit board was designed for assemble multiple LEDs on a board which is coated with biomaterial and to be implanted for light delivery. We expect this approach will increase the area of light emittance which would increase the photoconverted and photoactivated cells.

Results

The 405 nm LEDs successfully photoconverted the KikGR33 mouse cells and did not have any effect on the viability of the KikGR mouse model cells. Temperature changes of LEDs stayed well below tissue coagulation temperatures over time.

Comparison with Existing Method(s)

The LEDs did not damage mouse cells as previously done with the fiber optic cable and expected to have much better photoconversion/activation efficiency.

Conclusions

The LEDs successfully photoconverted KikGR mouse cells and was found to be within the photoactivation range of the Ai32 mouse cells. The LED-PCB is a safe and effective alternative to photoconvert and photoactivate immune cells which will aid the investigation of novel therapeutics for TB.

1. Introduction

1.1. TB current disease state and infection rates

Tuberculosis (TB) is a serious infectious disease that is among the top 10 causes of death globally, and is the leading cause of death from a single infectious agent [1]. Drug-resistant TB is a public health crisis with over half a million individuals developing TB with resistance to rifampicin, the most effective first line drug, and of those resistant, 82% had multiple drug resistant TB [1]. This clearly indicates a need for novel therapeutics to treat TB. A pathological hallmark of TB is granulomas, immune cell clustering around sites of infection, which is a potential target for therapy. Continuous cell replacement has been demonstrated as a mechanism of immune trafficking to maintain the granuloma microenvironment surrounding TB, however further research is needed in this area [2][3].

1.2. KikGR33 and Ai32 mouse models

They currently utilize two mouse models that express ion channels sensitive to light in their research: a KikGR33 mouse model which expresses green-red photoconvertible fluorescent protein at 405 nm and an Ai32 mouse model which expresses channelrhodopsins to allow photoactivation with exposed to 450 to 490 nm light (Fig. 1) [4]. Using a fiber optic cable, they illuminated small areas of affected tissue to photoconvert or photoactivate the cells. In KikGR mice, the lungs could then be excised up to seven days after photoconversion and examined to see the ratio of red immune cells that were photoconverted at the site to the green immune cells that were trafficked into the granuloma from unexposed tissue (Fig. 2) [2]. In Ai32 mice, calcium uptake by the cells can be observed to identify photoactivation.

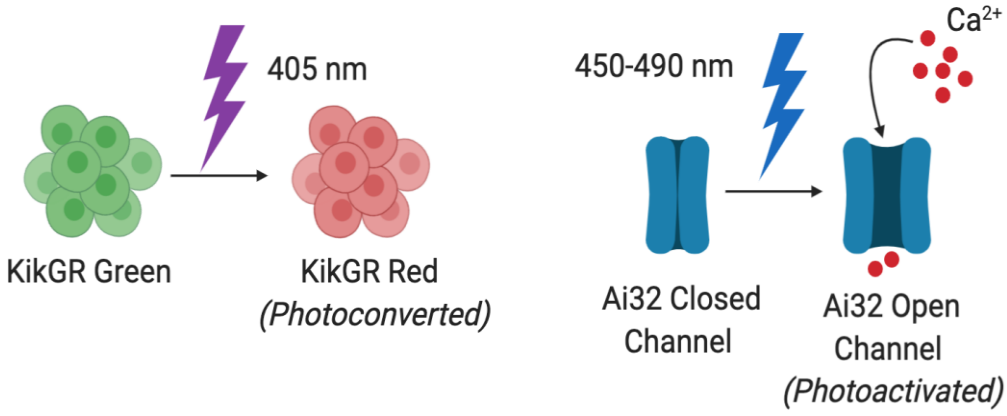

Figure 1. *The Sandor Lab uses two mouse models: KikGR which has photoconvertible cells when exposed to 405 nm wavelength and Ai32 which has photoactivatable cells that undergo calcium influx by channelrhodopsins after exposure to 450-490 nm light (Biorender).*

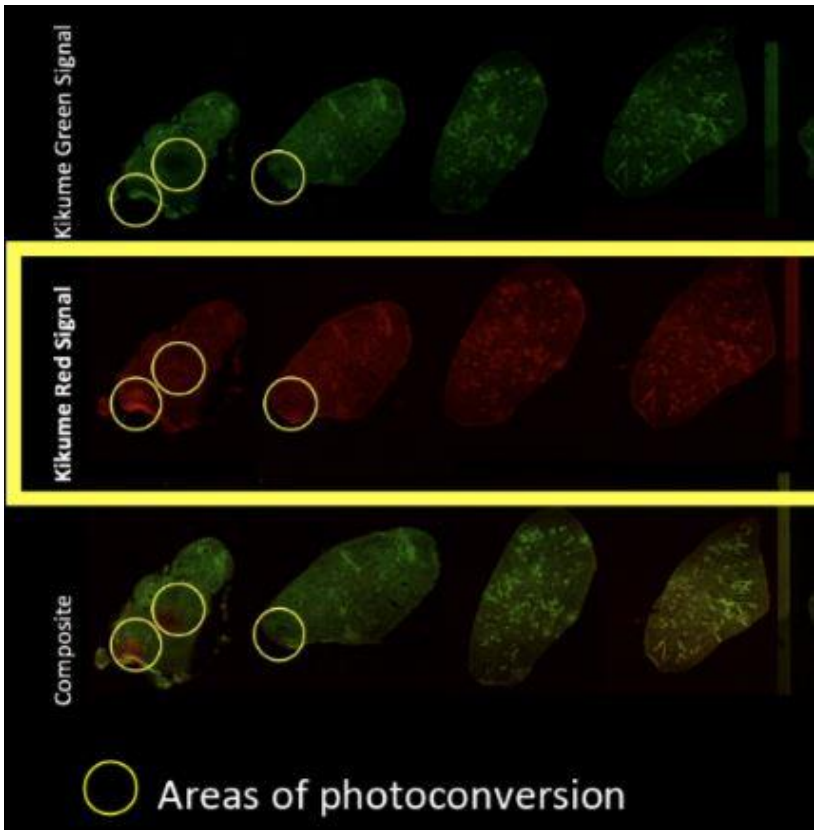

Figure 2: *Photoconversion by fiber optic cable is limited. Pictured above is fluorescent signalling from the lungs of KikGR33 mice infected with TB that had sites photoconverted by the fiber optic cable [2]. Note the small, inefficient area photoconverted (yellow circles).*

1.3. Significance of LED

Fiber optic cables are inefficient in photoconversion/photoactivation. An LED implantable device was designed, fabricated, and tested for its photoconversion and photoactivation efficiency with KikGR33 and Ai32 mouse cells. Our device will mitigate the disadvantages of other current methods by being biocompatible, effective at photoconverting a larger area, and cheap to manufacture. Furthermore, our device will have implications for other research areas that utilize optogenetics. The implantable device includes LEDs as a light source for photoconversion or photoactivation, design of the LED circuit, and a safe, biocompatible coating for our final product.

1.4. Design specifications

A light strength of 95 mw/cm^2 light source has been cited as effective for photoconverting tissues [5][6]. Dr. Matyas has specified that an area of approximately 1 cm^2 is needed to illuminate the mouse lung. The wavelength necessary for photoconversion of KikGR33 fluorescent protein used in the client's mouse model is 405 nm [4]. Another mouse model used is the Ai32 mouse that needs a 450 - 490 nm wavelength and 400 mW/cm^2 light strength to activate channelrhodopsins. Our client has requested that we develop a light source specific to the Ai32 mouse into a device as well. The light should limit photodamage and phototoxicity to the tissue. The implant should be biocompatible and must not trigger an immune response in the mouse. The design specifications are further summarized with a table for clarification (Table 1).

Table 1. *Summary of the design specifications for different functionalities.*

	Photoconversion	**Photoactivation**
Wavelength	405 nm	450 - 490 nm
Intensity	95 mW/cm^2	400 mW/cm^2
Size	1 cm^2	1 cm^2
Heat Output	< 2°C locally < 1°C systemically	< 2°C locally < 1°C systemically

The LEDs themselves must have the appropriate wavelength emission of 405 nm for successful photoconversion and 450-490 nm for photoactivation. The electronics must not cause excessive heat within the mouse. The Association for the Advancement of Medical Instrumentation (AAMI) recommended that an implant should not increase the systemic body temperature by more than 1°C and the local area should not increase by above 2°C [7]. Additionally, tissue coagulation will occur between 50°C and 60°C, so the implant must remain well below that temperature threshold [8].

Considerations for our biomaterial coating include optical clarity, biocompatibility, and electronic inertness. Common biomaterials used to encapsulate medical devices that are optically clear include silicones and parylenes. Parylene C is the gold standard for encapsulating electronic devices due to its optical clarity, high dielectric constant, and low permeability to water and chemicals [9][10][11]. Medical grade silicones can also be used for encapsulating devices, however their biocompatibility is less ideal than Parylene C [12].

There are devices available on the market for the photoconversion and photoactivation of KiKGR33 and Ai32 mouse cells. Devices used for photoconversion in previous scientific studies are the USHIO SP500 and SP250 spot UV curing equipment and Leica Microsystems fluorescence stereo microscopes (Fig. 3A) [5][6][13]. Prabhakar et. al [14] used a Fibertec II Fiber Coupled Diode Laser Module (Blue Sky Research) to photoactivate Ai32 mouse cells whereas Madisen et. al [15] used a 200-µm optical fiber coupled to a 593-nm yellow laser (Fig. 3B). Although these devices may already be on the market, none of them utilize LEDs as a source of light, these current devices can be expensive and are not as convenient to operate as LEDs.

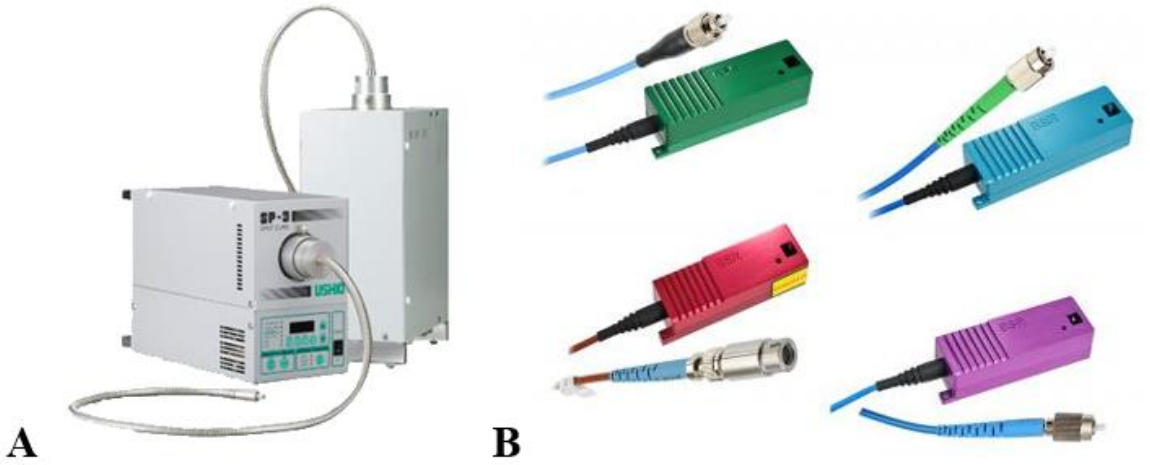

Figure 3: A, *The USHIO Spot-Cure Series, Spot UV Curing Equipment uses a low attenuation UV lamp [16].* ***B,*** *Blue Sky Research's FiberTec II™ Series uses fiber-coupled lasers that incorporate modulation and feedback functions [17].*

2. Materials and Methods

2.1. Electronics

405 and 480nm LEDs (Vishay Semiconductors, Malvern PA, USA and Changzhen Village, Guangming New District, Shenzhen, China) with solder mask defined pads (SMD) were purchased for the photoconversion and photoactivation of the KikGR33 and Ai32 mouse models respectively. The dimension of the 405nm LEDs is 3.2 mm x 2.8 mm x 1.9 mm and has a fixed wavelength and requires 20mA or 3.2V to operate [18]. The dimension of the 480nm 5050 RGB LEDs is 5mm x 5mm. It has an integrated driver chip and requires approximately 18mA constant current drive to operate [19]. The integrated driver chip allows additional functionalities to control the brightness, wavelength, and pulse width modulation using a NodeMCU ESP8266. The NodeMCU ESP8266 is compatible with the clockspeed used to control the 480nm LEDs.

2.2. Printed circuit board fabrication

A printed circuit board (PCB) was designed using *Altium Designer* (San Diego, CA), a commercial and electronic design automation software package for designing PCBs, to provide power and control to the LEDs. Two 405nm LEDs are connected in parallel to 3.3V (VCC) and ground (Fig. 4) to the microcontroller (MCU).

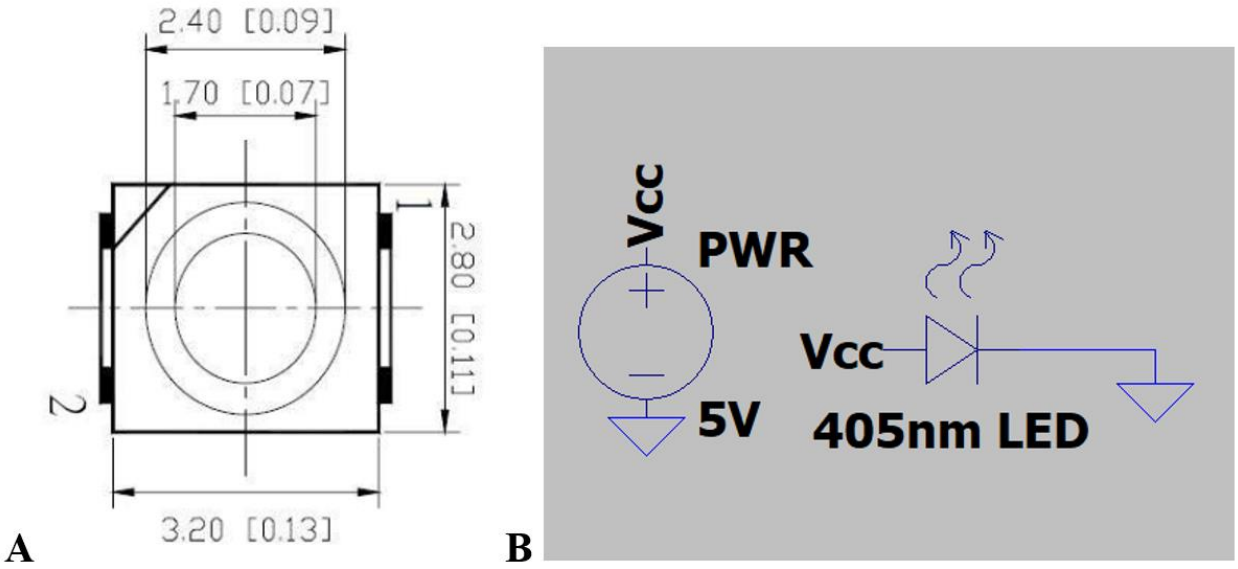

Figure 4: A, *The 405 nm LED is a 2 pin device, powered with 0-5 V (pin 1) and connected to ground (pin 2, units in mm) [18].* ***B,*** *LTSpice was used to create the circuit schematic. The PWR symbol represents a power supply of +5 V which is input into pin 1 of the LED represented by the triangle-vertical line symbol. It is then connected to the ground.*

Four 480nm LEDs are connected in parallel to provide the same amount of voltage to all LEDs (Fig.5). There are 4 pins on the 480 nm LEDs: pin 1 is for grounding the LED, pin 2 is used for control input signal data, pin 3 is for power supply, and pin 4 is for control output data. For the specification of the LED manufacturer, pin 4 of the previous LED must connect to pin 2 of the next LED for simultaneous control.The Ai32 mouse model PCB is designed to have one layer of ground, with 5V direct current supplied on the top layer (Fig. 6). The PCB designed fulfills the necessary connection requirement.

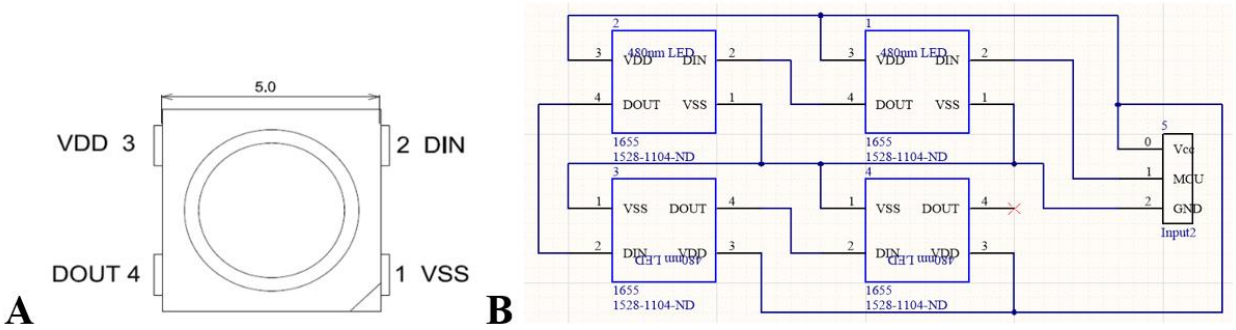

Figure 5. *The 480 nm LED is a 4 pin device. Pin 1 (VSS) is the ground pin, pin 2 (DIN) is the digital input pin that communicates with the microcontroller, pin 3 (VDD) is the power pin where +5 V is input, and pin 4 (DOUT) is the digital output pin where the LED can send the signal it receives from the microcontroller to other LEDs [19]. B, The 480 nm LEDs were powered in parallel (+5 V) through the Vcc pin of the microcontroller (represented by the Input2 symbol), connected to ground through the GND pin of the microcontroller, and the LED designator 1 communicated to the microcontroller (pin 2 LED to pin 1 of Input2).*

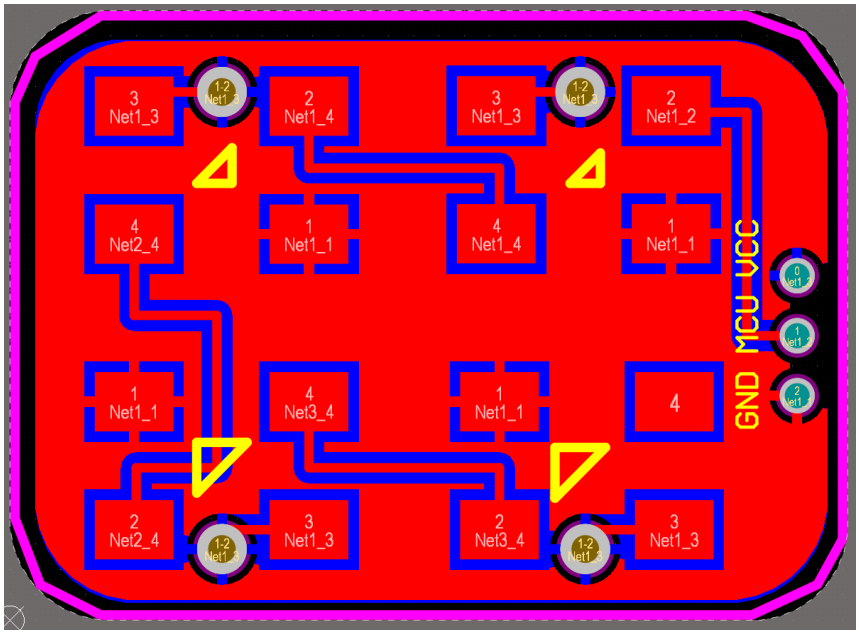

***Figure 6**. The PCB is designed for SMD pads with the LED connections on the top layer. The three pads on the far right are connected to the microcontroller to power, program, and ground the LEDs. Via connections are made so that the GND pads of the LEDs can access the second polygon pour connected to power.*

2.3. Arduino code

Code was developed on Arduino to allow users of the 480 nm LED to change the wavelength, brightness, and pulse width modulation using the serial monitor (Fig. 7). Within the code there is a wavelength to RGB conversion; however, the Neopixel only can simulate the appearance of a color with three different wavelengths: red, green, and blue. As a result, the wavelength used must rely solely on the blue pixel of the Neopixel and the code is currently being used to control the brightness and pulse width modulation of the blue pixel within the Neopixel. An advantage of incorporating pulse width modulation is that the LED will emit light at frequencies close to which the channelrhodopsins fire so that the channels are not exposed during their refractory period before they can fire again. The pulse width modulation will also conserve more energy since it is not powered constantly and will reduce phototoxicity and heat production.

```
[<pix_index>/c?<wavelenght(nm)>]
[<pix_index>/b?<brightness>]
[<pix_index>/f?<period(ms)>:<duty_cycle>:<cycles>]
```

Figure 7. *The format of the command input for Arduino.*

2.4. Testing

2.4.1. Wavelength and intensity

For wavelength and temperature testing an Ocean Optics Spectrophotometer (USB2000+) was used to collect wavelength and intensity data from the LEDs (Supplement X). In order to minimize saturation of the spectrophotometer, the LEDs were kept at a distance of 12 mm from the spectrophotometer (Fig. 8). Wavelength and intensity data was collected in triplicates to identify the consistency of the LEDs with standard error calculations and to identify the mean wavelength range and mean peak within the required intensity range for each of the LEDs (Fig. 8).

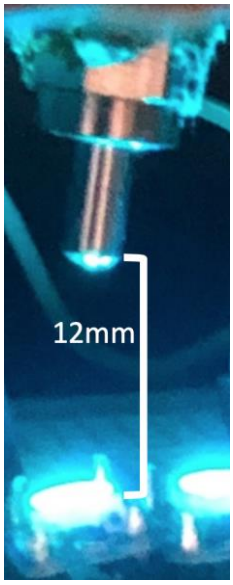

Figure 8*: The testing schema of light intensity using the Ocean Optics Spectrophotometer USB2000+.*

2.4.2. Temperature testing

Change in temperature of the LED *in vitro/in vivo* was simulated by measuring the change in temperature of phosphate-buffered saline (PBS) solution with the PDMS encapsulated PCB over a duration of two hours (Fig. 9).

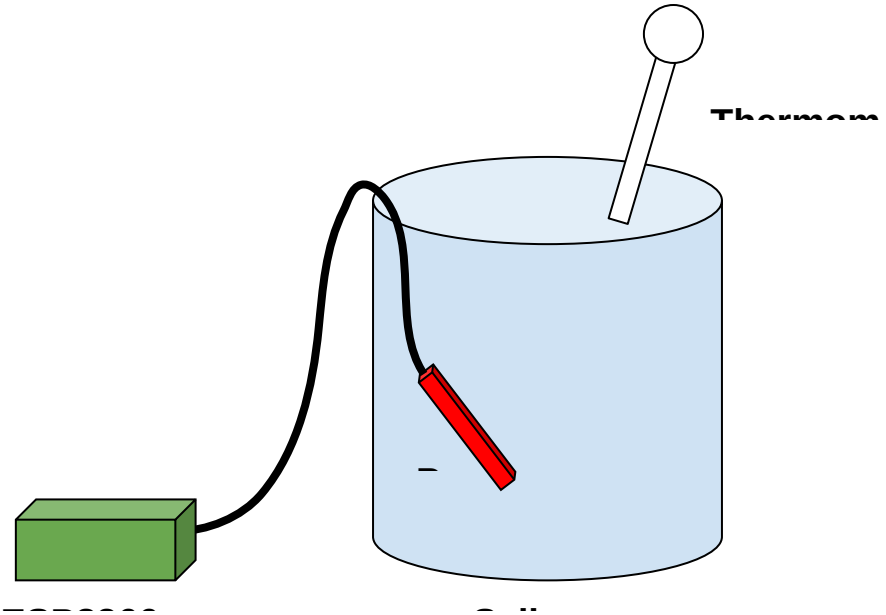

Figure 9. *The PDMS encapsulated PCB is placed in a saline solution and connected to the microcontroller. The starting temperature is 20°C (room temperature) and recorded every 10 minutes for two hours.*

The saline solution temperature was sampled every 10 minutes and then analyzed using *VassarStats*. Regression statistics were performed to identify the relationship and variation of temperature of the LEDs over time and to assess if it stayed below the temperature threshold.

2.5. In vitro testing

2.5.1. KikGR mouse model

A cell suspension of KikGR mouse lymph node cells were pelleted in a 1.7 mL clear, conical tube (Fig. 10A).The tube was placed on top of the 405 nm LED for 5 and 15 min with a 0 min exposure control (Fig. 10B). After exposure, the cells were resuspended, pipetted into a slide counter, and imaged under a confocal microscope. With no exposure to 405 nm wavelength light, the Kikume protein emits 517 wavelength light (green) under a fluorescent microscope when excited by a green laser (488 nm). With exposure of a 405 nm wavelength, the Kikume protein undergoes a conformational change and emit red (593 nm) when visualized under a fluorescent microscope after excitation with a red laser (594 nm). Cell viability was also assessed using Trypan blue following ~30 minutes after LED exposure.

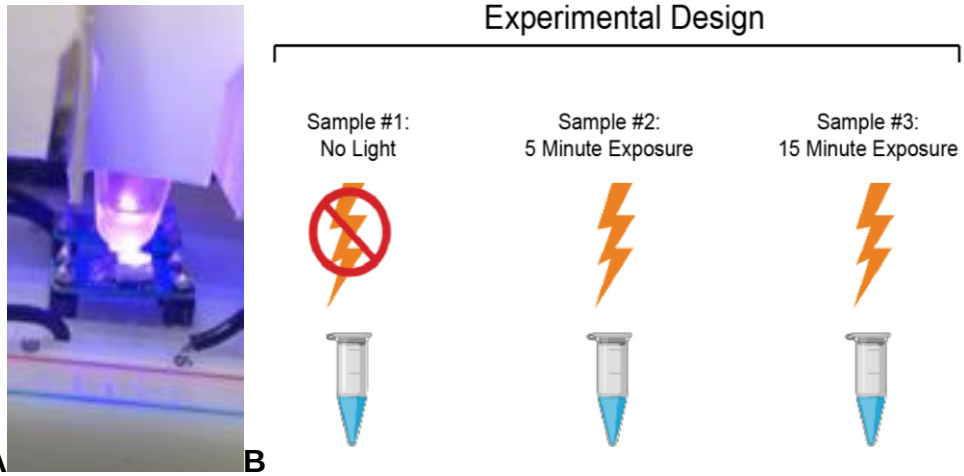

Figure 10: *In vitro testing of KikGR cells with 405 nm LED. A lymph node cell suspension of KikGR cells was pelleted in a 1.7 mL clear, conical tube and placed directly on the 405 nm LED (A) for 5 and 15 minutes with a 0 min exposure control (no exposure) (B).*

2.5.2. Ai32 mouse model

We will need to meet with our client to determine how they would like to measure Ai32 mouse models.

2.6. In vivo testing

Once the PCB has been confirmed to be functional and passes our tests above (especially the temperature, intensity, and wavelength tests), we will talk with our client on how to proceed with in *vivo testing*.

3. Results → <u>TO BE COMPLETED AS FURTHER VALIDATION REMAINS TO BE CARRIED OUT</u>

3.1. Device validation

3.1.1. LEDs meet Wavelength and Intensity Requirements

For the Blue LEDs, the mean lower bound wavelength at 400 mW/cm^2 was 449.9 nm (SE=4.02x10^{-14} nm) and the mean upper bound wavelength was 486.9 nm (SE =

0.1 nm). The peak wavelength and intensity was 465.2 nm (SE= 0 nm) and 520.73 mW/cm^2 (SE = 2.46 mW/cm^2) (Fig. 11). For the 405 nm LEDs, the mean lower bound wavelength at 95 mW/cm^2 was 392.2 nm (SE=0.1 nm) and the mean upper bound wavelength was 420.6 nm (SE = 6.96x10^{-14} nm). The peak wavelength and intensity was 405.7 nm (SE= 0.1 nm) and 501.9 mW/cm^2 (SE = 1.75 mW/cm^2) (Fig. 11).

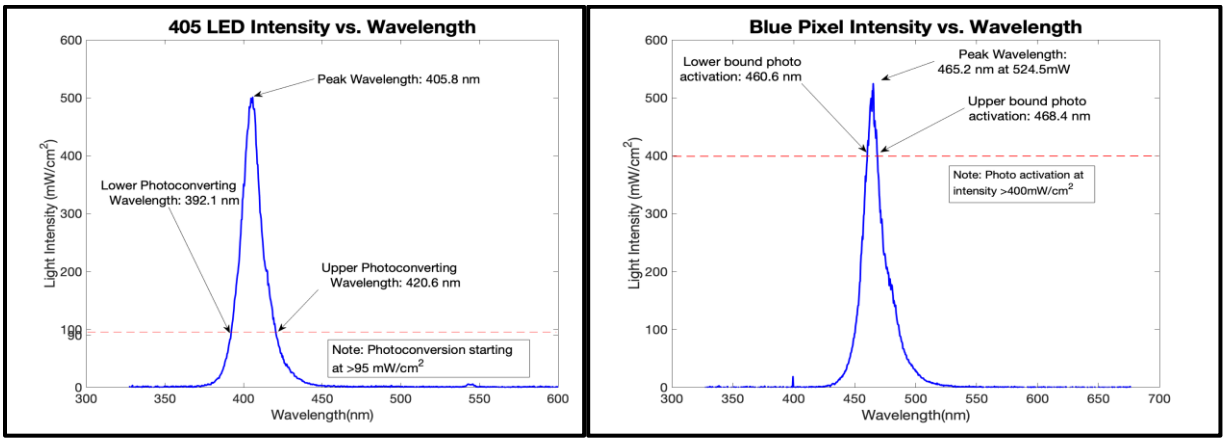

Figure 11. *Identifying photoconverting/activating wavelength range of LEDs. Device was tested in triplicates using Ocean Optics Spectrometer (USB2000+). The photoconvertible range of the 405 nm LED is on average from 392.2 nm and 420.6 nm with a peak wavelength at 405.8 nm and intensity of 501.9 mW/cm2. The blue LED photoactivating range is on average from 449.9 nm and 486.9 nm with a peak wavelength at 465.2 nm and intensity of 520.73 mW/cm2 (MATLAB).*

3.1.2. Temperature

DATA NOT YET ACQUIRED

3.1.3. PDMS/Parylene-C validation

DATA NOT YET ACQUIRED

3.2. In vitro photoconversion observed in 5 minute and 15 minute exposure groups

Photoconversion was observed with the 5 and 15 min exposure photoconverting the cells from green to red (Fig. 12A). The mean intensity of the 0 min exposure was on average 18.84 AU for KikGR green and 7.10 AU for KikGR red (standard deviation (std) = 4.92, standard error of the mean (SEM)=0.492 and std = 0.37, SEM=0.037 respectively). The exposed cells at 5 and 15 minutes showed on average 7.2 AU and 6.3 AU for KikGR green (std=0.57, SEM=0.057 and std=0.623 and SEM=0.06 respectively) and 22.98 AU and 22.49 AU for KikGR red (std = 4.85, SEM=0.485 and std=2.79, SEM=0.279 respectively) (Fig. 12B). In a two-way ANOVA the 5 and 15 minute exposure groups were significantly different from the 0 min exposure control

(p<0.0001). There was no statistically significant difference between the 5 minute and 15 minute exposure group. Cell viability assessed with trypan blue was shown to be unaffected between experimental groups shortly after exposure to the LEDs (Fig. 12C).

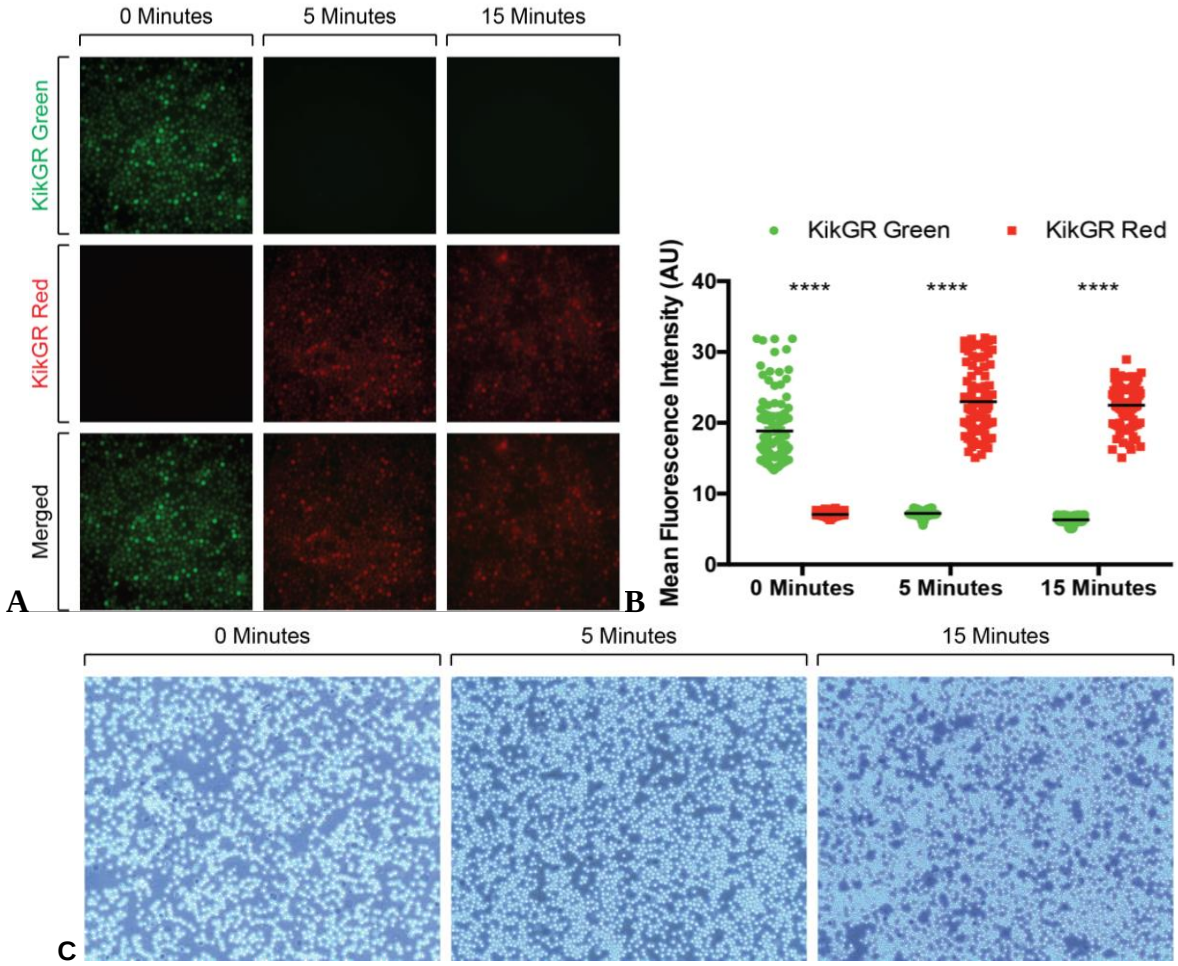

Figure 12: A-B, *Photoconversion of KikGR cells by 405 nm LED. The average mean fluorescence intensity in arbitrary units (AU) of 100 cells were measured using ImageJ, and quantified using Graphpad Prism. Two-way ANOVA, mean +/- s.e.m., n = 100 cells per group, **** p < 0.0001. No significant differences between 5 minute/15 minute groups.* ***C,*** *Cell viability, assessed with trypan blue, showed the LED had no immediate impact on cell viability.*

3.3. In vitro photoactivationn observed

DATA NOT YET ACQUIRED

3.4. Cell viability maintained after 24 hours from UV exposure

DATA NOT YET ACQUIRED

3.5. In vivo

DATA NOT YET ACQUIRED

4. Discussion → TO BE COMPLETED

Does it work? What are its limitations? What needs to be improved?

This portion will be completed when we have our tests and results analyzed.

[insert here author roles - For transparency, we encourage authors to submit an author statement file outlining their individual contributions to the paper using the relevant CRediT roles: Conceptualization; Data curation; Formal analysis; Funding acquisition; Investigation; Methodology; Project administration; Resources; Software; Supervision; Validation; Visualization; Roles/Writing - original draft; Writing - review & editing. Authorship statements should be formatted with the names of authors first and CRediT role(s) following → from their journal author guidelines] ****copy and pasted from the journal's guidelines**

5. Acknowledgements

Our team would like to thank Dr. Williams & Dr. Amit Nimunkar for their guidance, Dr. Sandor's Lab for providing us the opportunity to work on this project, and Hayden Pilsner & Thomas Debroux II for code consultation.

6. References

[1] "Global tuberculosis report 2018," World Health Organization, 11-Sep-2019. [Online]. Available: https://www.who.int/tb/publications/global_report/en/. [Accessed: 08-Oct-2019]. https://www.nationalgeographic.org/encyclopedia/bioluminescence/. [Accessed: 10-Oct-2018].

[2] S. A. Marcus, M. Herbath, Z. Fabry, and M. Sandor, "Dynamic changes in Mycobacterium tuberculosis-induced granulomas: developing new tools," The Journal of Immunology, 01-May-2018. [Online]. Available:https://www.jimmunol.org/content/200/1_Supplement/117.19. [Accessed: 08-Oct-2019].

[3] C. Bussi and M. G. Gutierrez, "Mycobacterium tuberculosis infection of host cells in

space and time,” FEMS microbiology reviews, 01-Jul-2019. [Online]. Available: https://www.ncbi.nlm.nih.gov/pmc/articles/PMC6606852/. [Accessed: 08-Oct-2019].

[4] “STOCK Tg)CAG-KikGR)33Hadj/J Overview,” 013753 - STOCK Tg(CAG-KikGR)33Hadj/J. [Online]. Available: https://www.jax.org/strain/013753. [Accessed: 08-Oct-2019].

[5] M. Tomura, A. Hata, S. Matsuoka, F. H. W. Shand, Y. Nakanishi, R. Ikebuchi, S. Ueha, H. Tsutsui, K. Inaba, K. Matsushima, A. Miyawaki, K. Kabashima, T. Watanabe, O. Kanagawa, "Tracking and quantification of dendritic cell migration and antigen trafficking between the skin and lymph node," Scientific Reports, vol. 4, no. 6030, Aug. 2014. [Online] Available: https://www.ncbi.nlm.nih.gov/pmc/articles/PMC4129424/

[6] M. Tomura, N. Yoshida, J. Tanaka, S. Karasawa, Y. Miwa, A. Miyawaki, O. Kanagawa, "Monitoring cellular movement in vivo with photoconvertible fluorescence protein "Kaede" transgenic mice," Proceedings of the National Academy of Sciences of the United States of America, vol. 105, no. 31, pp. 10871-10876. [Online]. Available: https://www.ncbi.nlm.nih.gov/pmc/articles/PMC2504797/

[7] Reichert, W. (2008). Indwelling Neural Implants: Strategies for Contending With the in Vivo Environment (Frontiers in neuroengineering). CRC Press, Chapter 3.

[8] J. Heisterkamp, R. van Hillegersberg, J.N. Ijzerman. (1999). Critical temperature and heating time for coagulation damage: implications for interstitial laser coagulation (ILC) of tumors. Lasers in Surgery and Medicine. Available at: https://www.ncbi.nlm.nih.gov/pubmed/10495303

[9] S. Hornm "Silicone Conformal Coating vs. Parylene," Diamond-MT, Conformal Coating, August. 7, 2015. [Online]. Available: https://blog.paryleneconformalcoating.com/silicone-conformal-coating-vs-parylene. [Accessed: December 9, 2019].

[10] S. Ahn, J. Jeong, S. J. Kim, "Emerging Encapsulation Technologies for Long-Term Reliability of Microfabricated Implantable Devices," Micromachines (Basel), vol. 10, no. 8, pp. 508. 2019. [Online]. Available: https://www.ncbi.nlm.nih.gov/pmc/articles/PMC6723304/

[11] Specialty Coating Systems (2007) "Parylene Properties," Specialty Coating Systems. [Online] Available: https://www.physics.rutgers.edu/~podzorov/parylene%20properties.pdf. [Accessed: December 10, 2019].

[12] D. S. Lee, S. J. Kim, E. B. Kwon, C. W. Park, S. M. Jun, B. Choi, S. W. Kim, "Comparison of in vivo biocompatibilities between parylene-C and polydimethylsioxane for implantable microelectronic devices," Bulletin of Materials Science, vol. 36, no. 6, pp. 1127-1132. [Online]. Available: https://www.ias.ac.in/article/fulltext/boms/036/06/1127-1132

[13] M. Tomura, T. Honda, K. Tanizaki, A. Otsuka, G. Egawa, Y. Tokura, H. Waldmann, S. Hori, J. G. Cyster, T. Watanabe, Y. Miyachi, O. Kanagawa, K. Kabashima, "Activated regulatory T cells are the major T cell type emigrating from the skin during a cutaneous immune response in mice, " The Journal of Clinical Investigation, vol. 120, no. 3, pp. 883-893. [Online]. Available: https://www.ncbi.nlm.nih.gov/pmc/articles/PMC2827959/

[14] A. Prabhakar, D. Vujovic, L. Cui, W. Olson, W. Luo, B. Arenkiel, "Leaky expression of channelrhodopsin-2 (ChR2) in Ai32 mouse lines," PLOS One, vol. 14, no. 3. [Online]. Available: https://www.ncbi.nlm.nih.gov/pmc/articles/PMC6435231/

[15] L. Madisen, T. Mao, H. Koch, J. Zhuo, A. Berenyi, S. Fujisawa, Y. A. Hsu, A. J. Garcia III, X. Gu, S. Zanella, J. Kidney, H. Gu, Y. Mao, B. M. Hooks, E. D. Boyden, G. Buzsaki, J. M. Ramirez, A. R. Jones, K. Svoboda, X. Han, E. E. Turner, H. Zeng, "A toolbox of Cre-dependent optogenetic transgenic mice for light-induced activation and silencing," Nature Neuroscience, vol. 15, no. 5, pp. 793-802. [Online]. Available: https://www.ncbi.nlm.nih.gov/pmc/articles/PMC3337962/

[16] USHIO, Deep UV Lamp Spot-Cure Series - Spot UV Curing Equipment, Tokyo Instruments, 2019. Accessed on: December. 9, 2019. [Online]. Available: http://www.tokyoinst.co.jp/en/products/detail/UD02/index.html

[17] Blue Sky Research, Fiber Coupled Lasers, Blue Sky Research, 2019. Accessed on: December. 9, 2019. [Online]. Available: https://blueskyresearch.com/products/fiber-coupled-lasers-and-systems/fiber-coupled-lasers/

[18] Mouser Electronics. (2020). VLMU3100-GS08 Vishay Semiconductors | Mouser. [online] Available at: https://www.mouser.com/ProductDetail/Vishay-Semiconductors/VLMU3100-GS08?qs=sGAEpiMZZMsl8UZd3ZuU6YZ3nvPDyevX9oPcBaE1QHc%3D [Accessed 26 Feb. 2020].

[19] Industries, A. (2020). NeoPixel 5050 RGB LED with Integrated Driver Chip - 10 Pack. [online] Adafruit.com. Available at: https://www.adafruit.com/product/1655 [Accessed 26 Feb. 2020].

7. Supplementary Data/Figures:

7.1. Wavelength and Intensity Calculations

For the LED intensity and wavelength testing, the data had to be further analyzed because the USB 2000+ gives a light intensity measured in counts every 100ms, and for our purposes intensity should be in units of mW/cm^2. Every count of photon energy is calculated with $h * c/\lambda$ where h is Planck's constant, c is the velocity of light, and λ is the wavelength measured (Equation 1). Since the counts are measured within 100ms, the number of counts in one second is 10 times more than the counts in 100 ms. The USB2000+ has a light sensitive array with 2048 pixels which is 14μm x 200μm [6]. Then, the light intensity within a certain area may be calculated by the light energy divided by the pixel area (Equation 2).

$$E = counts * \frac{1s}{100ms} * \frac{h * c}{\lambda} \qquad \textbf{\textit{Equation (1)}}$$

$$light\ intensity\ per\ area = \frac{E}{Area} \qquad \textbf{\textit{Equation (2)}}$$

By using these 2 equations, the spectrophotometer intensity data could be converted into the light intensity units of mW/cm^2.